Secretome of EMSCs neutralizes LPS-induced acute lung injury via aerosol administration

JIANING TAN[1], ZILIANG ZHUO[1], XIUYU WANG[1], YANSHUANG ZHANG[1], YUCHENG QIAN[1] and FANGFANG LIN[2]

[1]Department of Neurology, Changshu No. 2 People's Hospital, Affiliated Changshu Hospital of Nantong University, Changshu, Suzhou 215500; [2]Department of Oncology, The First People's Hospital of Zhenjiang, Affiliated Hospital of Jiangsu University, Zhenjiang, Jiangsu 212000, P.R. China

Received June 1, 2023; Accepted September 4, 2023

DOI: 10.3892/ijmm.2023.5307

Abstract. Ectodermal mesenchymal stem cells (EMSCs) are cells harvested from the stem cell niche (nasal mucosa) with high therapeutic potential. To the best of our knowledge, however, the anti-inflammatory properties of these neural crest-derived EMSCs have been rarely reported. The present study aimed to explore the effects of aerosolized EMSC-Secretome (EMSC-Sec) and clarify underlying mechanisms in treating acute lung injury (ALI). EMSCs were isolated by adherent method and identified by immunofluorescence staining. EMSC-Sec was collected and evaluated using western blotting, BCA and ELISA tests. Then, mouse lung epithelial cells (MLE-12) were used to mimic inflammatory stimulation with lipopolysaccharide (LPS). After developing an ALI model through intraperitoneal injection of LPS, mice were treated with an EMSC-Sec spray. The lung in each group underwent an observation and measurement to preliminarily assess the extent of damage. H&E staining, immunohistochemical staining, immunofluorescence and western-blotting were utilized to further access the impacts of EMSC-Sec. The results showed that EMSC-Sec had great anti-inflammatory potential and was highly successful *in vitro* and *in vivo*. EMSC-Sec mitigated LPS-induced ALI with low inflammatory cell inflation and mild damage. EMSC-Sec could regulate inflammation via the NF-κB(p50/p65)/NLRP3 pathway. Overall, the present study demonstrated that EMSC-Sec regulated inflammation, hoping to provide a novel strategy for ALI treatment.

Correspondence to: Ms. Jianing Tan, Department of Neurology, Changshu No. 2 People's Hospital, Affiliated Changshu Hospital of Nantong University, 18 Taishan Road, Changshu, Suzhou 215500, P.R. China
E-mail: janietjn@163.com

Dr Fangfang Lin, Department of Oncology, The First People's Hospital of Zhenjiang, Affiliated Hospital of Jiangsu University, 8 Dianli Road, Runzhou, Zhenjiang, Jiangsu 212000, P.R. China
E-mail: 2534409923@qq.com

Key words: acute lung injury, ectodermal mesenchymal stem cell, secretome, NLRP3

Introduction

Sepsis is a life-threatening organ dysfunction, causing 11 million deaths yearly (1,2). Sepsis-induced acute lung injury (ALI) is a common complication causing 74,500 deaths/year in Europe and the United States (3-5). Due to rapid onset of widespread inflammation and acute epithelial cell injury in the lungs, severe respiratory syndrome and symptoms occur, including shortness of breath, rapid breathing and bluish skin coloration (6). Though some conventional treatments including mechanical ventilation and fluid management based on the underlying diseases and clinical care relieve symptoms, high morbidity and mortality of ALI are a significant challenge requiring novel therapeutic options.

Mesenchymal stem cells (MSCs) could modify pathophysiology, regulate immunization and support tissue regeneration (7,8). MSCs also have been researched in inflammatory disease for their multifunctionality (9,10). Specifically, studies have highlighted the therapeutic applications of MSCs in Coronavirus disease 2019 (COVID-19) by inhibiting inflammatory cytokine storm (11,12). However, the mechanism by which MSCs play their functions is unknown. It is hypothesized that the therapeutic effects are mediated by cell communications and the replacement of MSCs (13,14). Therapy based on MSCs replacement is hindered by the harsh microenvironment in the site. Theoretically, the rationale for treatment may primarily relied on MSCs-activated cell-to-cell communication by paracrine effects to improve niche via delivering signals to endogenous cell (15-17). Immunomodulation in innate and adaptive immune systems is mediated by the secretome (Sec) of MSCs (18). The Sec, containing cytokines, chemokines and extracellular vesicles (EVs) directly regulates the microenvironment to achieve immunological balance (19). Using Sec from MSCs is a therapeutic strategy for inflammatory disease. Ectodermal (E)MSCs, a type of MSC developed from neural crest (NC), are extensively obtained from nasal mucosa without direct invasive injury and have potential clinical applications. Simultaneously, potent tissue regeneration potential makes EMSCs a candidate as seed cells (20,21). Thus, EMSC-Sec deserves further investigation in inflammation.

NF-κB(p50/p65) is a crucial molecular driver of the inflammatory response (22). Under physiological conditions,

most NF-κB(p50/p65) dimers exist with an inactive state in the cytoplasm because of binding of inhibitors (IκB). However, pathological changes frequently trigger pattern recognition receptor and antigen receptor-mediated signaling cascades and activate the IκB kinase (IKK) complex. Phosphorylation of IκB results in ubiquitination and degradation of IκBα by proteases, allowing NF-κB(p50/p65) to be translocated to the nucleus (23). NF-κB(p50/p65) initiates gene transcription, increases expression of inflammatory factors, including Nod-like receptor thermal protein domain associated protein 3 (NLRP3) (24), and promotes inflammatory cytokine cascade. This cascade caused by NLRP3-dependent pyroptosis, a type of programmed death, triggers inflammation by extensively releasing cell content (25,26). Hence, regulating the NF-κB(p50/p65)/NLRP3 pathway is crucial to improve inflammation.

Atomized drugs are a user-friendly means of administering medication and could maintain efficacious concentrations of drugs at different sites in the lung, allowing the drug to penetrate readily through the lung mucosa to the blood supply (27). Aerosolization of immunotherapeutic agents has potential to manipulate the local mucosal-specific microenvironment (28). Compared with intratracheal administration, the delivery of drugs via a mucosal atomization device could be more likely to achieve therapeutic concentrations with pharmacokinetic effect (29). The present study used aerosolization to ameliorate inflammation utilizing EMSC-Sec. It was hypothesized that EMSC-Sec in the gaseous form restores the inflammatory microenvironment. The present study aimed to explore the anti-inflammation capabilities of EMSC-Sec in ALI and elucidating the underlying mechanism.

Materials and methods

Extraction and identification of EMSCs. EMSCs were collected using a tissue adhesion method as previously described (30). A total of five 3-week-old (30 g) male rats (Jiangsu University Animal Center) were sacrificed by intraperitoneal sodium pentobarbital overdose (200 mg/kg). Experiments were performed ~10 min after cessation of breathing. The nasal septum was removed after disinfection with iodine. The nasal mucosa was cut into 1 mm thick pieces on ice after washing with PBS. Tissue was suspended in DMEM/F12 containing 10% fetal bovine serum (FBS, both HyClone; Cytiva). The suspension was transferred to a plate at 37˚C for cultivation for 3 days. Cells at 80% confluence were subsequently subcultured following trypsin digestion. EMSCs at three passages were identified by detection of surface markers CD44, Connexin 43 (Cx43), SRY-related high-mobility group box-containing protein 9 (Sox9) and vimentin (all of antibodies purchased from Wuhan Boster Biological Technology, Ltd.) with immunofluorescent staining. The study protocol was approved by the Animal Care and Use Committee of Jiangsu University (Zhenjiang, China).

Preparation and analysis of EMSC-Sec. The EMSCs (passage 3) were used. After the cell confluence reached 80%, the complete medium containing 10% FBS was replaced with DMEM/F12 with FBS (1%) at 37˚C for 24 h. EMSCs were cultured in complete medium at 37˚C with 5% CO_2 for another 24 h. This process was repeated for at least 10 times to accumulate EMSC-Sec. A total of 50 ml EMSC-Sec was centrifuged at 2,000 x g at 4˚C for 10 min to remove non-adherent cells and cellular debris. The supernatant was collected and concentrated by lyophilized method (31). Then, 5 ml EMSC-Sec concentrate derived from 50 ml EMSC-Sec was evaluated by BCA tests. Immunosuppressive agents (IL-10, TGF-β), neurotrophic factors (Sonic hedgehog, SHH), and bioactive substances (EVs) have emerged as pivotal factors in the regulation of the inflammatory microenvironment (32-35). Proteins were analyzed using western blot to determine whether EMSC-Sec possesses therapeutic potential. ELISA test was conducted to assess the levels of IL-10 in EMSC-Sec.

Evaluation of EMSC-Sec in vitro. LPS is used to construct inflammatory cell models as previously reported (36). MLE-12 cells (Feng Hui Biological Co., Ltd.) were cultivated in high-glucose DMEM (HyClone, Cytiva) supplemented with 10% FBS. MLE-12 ($1x10^6$ cells/ml) in the culture plate were exposed to 10 μg/ml LPS (Macklin Biology Co., Ltd.) at 37˚C for 24 h to establish a cell model. To confirm whether EMSC-Sec alleviates inflammatory injuries, cells were treated with EMSC-Sec (0, 4, 6, 8 mg/ml) following LPS intervention at 37˚C for 48 h.

Cell Counting Kit-8 (CCK-8) kit purchased from Macklin company were adopted to evaluate viability. The LPS challenged MLE-12 cells after EMSC-Sec treatment (0, 4, 6, 8 mg/ml) were incubated with CCK-8 in an incubator containing 5% CO_2 at 37˚C for 30 min. Then, data was detected and analyzed at 450 nm by the microplate reader.

Animal model and experimental design. A total of 40 male C57BL/6 mice (25 g, 8 weeks) were purchased from Henan Sikebeisi Biotechnology Co., Ltd. Following 3 days adaptive feeding with enough food and water in an appropriate environment (temperature, 24-27˚C; humidity, 40-50%; light-dark cycle, 12-12 h), the mice were randomized into four groups: Control, LPS, EMSC-Sec and LPS + EMSC-Sec (n=10/group). ALI model was constructed by injecting 200 μl LPS dissolved in PBS (20 mg/kg) intraperitoneally for 24 h (37,38). Mice in the EMSC-Sec group without LPS challenge and LPS + EMSC-Sec group received 4 mg/ml EMSC-Sec once treatment before and after LPS injection. The first treatment was performed using an atomizer (Omron Co., Ltd.) 6 h ago before LPS injection. The second treatment was performed immediately following LPS treatment using the same atomizer. Multiple mice were placed in the atomizer for each administration. Subsequently, 20 ml EMSC-Sec (4 mg/ml) was delivered six times at 6 h intervals between each intervention until the mice were sacrificed in EMSC-Sec group and LPS+EMSC-Sec group. The health of mice was monitored every 6 h by observing the fur, behavior and hogback performance. In light of the LPS-induced ALI causing multiple organ failure, we considered humane endpoints, which included noticeable arching of the back and reduced behavioral activity.

Mice in each group (n=3) were euthanized by intraperitoneal injection of sodium pentobarbital (50 mg/kg). Then, 1 ml blood sample was immediately extracted from the left ventricle. To enhance the assessment of the impact, the lung, spleen, and

liver from each group of mice were excised for morphological observation. All procedures were in accordance with the animal research institute guidance and ethical standards of Jiangsu University (approval no. UJS-IACUC-2022051901).

Wet/dry (W/D) lung weight ratio. Lung samples were collected and weighed (wet weight), then dried in an oven at 60˚C for 24 h to measure dry weight. Tissue edema was evaluated using the W/D ratio.

ELISA. IL-10 in EMSC-Sec was analyzed by ELISA (cat. no. EK0417, Wuhan Boster Biological Technology, Ltd.) following the manufacturer's instructions. The blood samples were centrifuged at 12,000 x g at 4˚C for 5 min. The murine serum was prepared for the detection of IL-10 and TNF-α. The optical density was measured at the wavelength of 450 nm using a microplate reader.

Histopathology in pulmonary tissue. Lung tissues were collected and fixed with 4% paraformaldehyde at 4˚C overnight. Samples were embedded in paraffin and then sectioned (thickness, 4 μm). Next, slices were incubated with xylene solution for 20 min. Then, a sequential cleaning was performed using anhydrous ethanol, followed by 95, 85, 75% ethanol, and Double Distilled Water (ddH_2O) for a duration of 5 min. The samples were subjected to 0.01 M citrate buffer incubation in a microwave oven at 92 to 98˚C for a duration of 10 min to retrieve antigens. The slices were submerged in a 3% hydrogen peroxide solution and left to incubate at room temperature (RT) in a light-protected environment for 25 min, followed by three rinses with PBS. The tissue was uniformly coated with a 3% BSA solution and left to incubate at RT for 30 min. Following that, we applied the primary antibody IL-17 (1:100, obtained from Boster, catalog number A00421-2) to incubate the tissue slices at 4˚C overnight. Following PBS washing, the tissue was subsequently treated with an HRP-labeled secondary antibody and incubated at RT for 1 h. Ultimately, the color was induced using a DAB chromogenic solution. The DAB Kit, which includes a secondary antibody and DAB solution, was acquired from Boster (AR1027-3). The pictures were captured using a light microscope at magnifications of x100 and x200.

Subsequently, the sections were stained with hematoxylin and eosin (H&E) to determine pathological changes. The sections were immersed in hematoxylin solution for 5 min at room temperature (RT) to stain the cell nuclei, followed by water washing. It is then briefly subjected to 1% hydrochloric acid alcohol differentiation and rinsed in tap water. Next, the slides were submerged in eosin solution for 2 min at RT to stain the cytoplasm and other tissue components. The severity of the lung injury was evaluated by infiltration of the inflammatory cells, the degree of swelling and the thickness of the alveolar partition in at least three randomly selected fields of view. Lung injury was scored on a scale of 0 to 5 (39) as follows: 0, no damage; 1, injury covering 1-10% of the area; 2, injury covering 11-25% of the area; 3, injury covering 26-50% of the area; 4, injury covering 51-75% of the area and 5, injury covering >75% area. Qualitative hematoxylin and eosin (H&E) staining was performed for observation under a light microscope at a magnification of 100 and 200. Images were analyzed with GraphPad Prism 8 (GraphPad Software, Inc.; Dotmatics).

Western blotting. Lung tissues were homogenized and lysed in RIPA buffer containing cocktail inhibitors (Sigma-Aldrich; Merck KGaA) and centrifuged at 4˚C and 12,000 g for 10 min. The protein concentration was detected with bicinchoninic acid kit (Sango Biotech). A total of 10 microliters of protein samples were loaded per lane, and electrophoresis was conducted under a constant voltage of 80V. Polypeptides were separated by 10% SDS-PAGE. The protein bands in gel were electrically transferred to polyvinylidene fluoride membranes (MilliporeSigma) for 100 min using a constant current of 350 mA. The membranes were blocked with 5% Bovine Serum Albumin (BSA, Macklin) at RT for 1 h and then incubated with anti-SHH (1:500, Boster, A00058-1), anti-Toll-like receptor 4 (TLR4) (1:500, Boster, A00017-3), anti-MPO (1:500, Boster, BA0544), anti-IL-10 (1:2,000, Proteintech, 60269-1-Ig), anti-IL-1 (1:500, Boster, A00101-1), anti-TNF-α (1:500, Boster, cat. no. BA0131), anti-NF-κB (p50/p65; 1:500, Boster, A00284-1), anti-IκB (1:500, Boster, PB9291), anti-phosphorylated (p-)IκB (1:500, Boster, P01139-1), anti-NLRP3 (1:500, Boster, A00034-2) and anti-β-actin (1:500, Boster, BA2305) antibodies at 4˚C overnight. Blots were washed three times with TBS containing 0.1% Tween-20 and incubated with horseradish peroxidase-conjugated secondary antibody (1:5,000, Boster, BM3894) for 1 h at room temperature. Finally, protein expression levels were measured by enhanced chemiluminescence kit (Millipore, Sigma). All of the bands were analyzed by ImageJ software (National Institutes of Heath).

For cell samples, the cells were subjected to western blot analyses after stimulation. Briefly, MLE-12 cells were collected with a chemical lysis method (40). After loading the boiled protein, the antibodies of IL-10 and TNF-α were applied to the detection and eventually analyzed by ImageJ software.

Immunofluorescence. Cells or tissues were fixed in 4% paraformaldehyde. The tissue samples were embedded in paraffin and cut into slices with a thickness of 4 μm. After 30 min in a 60˚C oven, the slices were subjected to low-grade alcohol dewaxing and then hydration, following the above-described method in the text. Then, the samples were subjected to a 0.01M citrate buffer incubation in a microwave oven at temperatures ranging from 92 to 98˚C for a duration of 10 min to retrieve antigens. Next, the cell membrane was permeabilized by 0.1% Triton-100 at RT for 10 min. After three washes with PBS, 5% BSA was adopted to block the protein at 37˚C for 30 min. Then, the sections were exposed to a mixture solution comprising IL-10 (1;100, Proteintech, Inc.; 60269-1-Ig) and TNF-α (1:100, Boster, BA0131) and were kept at 4˚C overnight. Following three PBS washes, the samples were also exposed to a mixture solution including CY3-labeled goat-anti-rabbit (1:100, Boster, BA1032) and CY3-labeled goat-anti-mouse (1:100, Boster, BA1031) antibodies in a dark, humid environment at 37˚C for 60 min. The nucleus was stained by DAPI (Beijing Solarbio, C0065) at RT for 10 min.

For cell samples, procedure of immunofluorescence is also same. Briefly, samples in 24-well plates were incubated with primary antibodies for CD44 (1:100, Boster, A00052),

Cx43 (1:100, Boster, BA1727), Sox9 (1:100, Boster, PA1026-1), Vimentin (1:100, Boster, PB9359) after being blocked with BSA. Following that, CY3-labeled goat-anti-rabbit (1:100, Boster, BA1032) antibody and DAPI was adopted. The fluorescence was determined at a magnification of 100 and x200 under a Nikon fluorescence microscope (TE200-U). The data was analyzed using Image J software.

Statistical analysis. All data derived from three independent experimental repeats are presented as the mean ± SEM. Statistical analysis was performed with SPSS 19.0 software (SPSS Inc.). One-way ANOVA followed by Tukey's post hoc test was adopted to determine the statistical significance. $P<0.05$ was considered to indicate a statistically significant difference.

Results

Characterization and identification of EMSCs. Primary EMSCs (P0) proliferated after 3 days of culture in DMEM/F12 containing 20% FBS (Fig. 1A). Prolonged cultivation over three generations of purified EMSCs is depicted on the right side of Fig. 1A. The immunofluorescence results revealed that EMSCs expressed MSC markers (CD44, Cx43). Also, positive staining of the biomarker of NC stem cells (Cx43) and NC-related marker (Sox9) in EMSCs revealed that EMSCs originated from NC SCs (Fig. 1B).

Components of EMSC-Sec. To determine the potential role of EMSC-Sec in inflammation and recovery, the present study evaluated the expression of anti-inflammatory cytokines (IL-10, TGF-β), trophic factor (SHH) and exosome markers (CD9, CD63) in concentrated EMSC-Sec. The data in Fig. 2A showed that EMSC-Sec may be therapeutic in inflammatory diseases. In addition, BCA and ELISA were performed to quantify protein and cytokines in EMSC-Sec. The concentration of EMSC-Sec lyophilized powder in a 10-fold dilution was approximately 20 mg/ml, aligning with the findings observed for EMSC-Sec at 2 mg/ml (as shown in Fig. 2B). IL-10 holds a pivotal position in regulating inflammation, influencing the course and progression of inflammatory diseases (33). A total of 320 pg/ml IL-10 was present in concentrated EMSC-Sec, indicating the potential of EMSC-Sec to regulate inflammation.

Role of EMSC-Sec in MLE-12 following LPS challenge. MLE-12 cells in good condition were cultured on 6-well plates. As shown in Fig. 3A, MLE-12 displayed a fibroblastic appearance and clustered into formations resembling petals. LPS-exposed MLE-12 cells were rescued using enriched EMSC-Sec (Fig. 3C). To verify the influence of EMSC-Sec, the present study conducted western blotting (Fig. 3B). The LPS+EMSC-Sec group (4, 6, 8 mg/ml) expressed lower levels of TNF-α than the LPS group, suggesting a significant anti-inflammatory effect in the LPS+EMSC-Sec group (Fig. 3F). Likewise, elevated expression of IL-10 showed that EMSC-Sec regulated inflammation (Fig. 3G). The ELISA outcomes depicted in Fig. 3D and E also confirm that EMSC-Sec elevate the expression of IL-10 and modulate the regulation of TNF-α. Above data showed that 4 mg/ml EMSC-Sec inducing immune equilibrium via up-expression of IL-10 (Fig. 3E and G). Additionally, EMSC-Sec promoted proliferation (Fig. 3H). After exposure to LPS (10 μg/ml), MLE-12 cells exhibited a swift increase in activity before the 12-h mark. However, between the 12 and 24th h, the secretion from EMSCs significantly promoted the proliferation of MLE-12 cells, particularly at a concentration of 4 μg/ml.

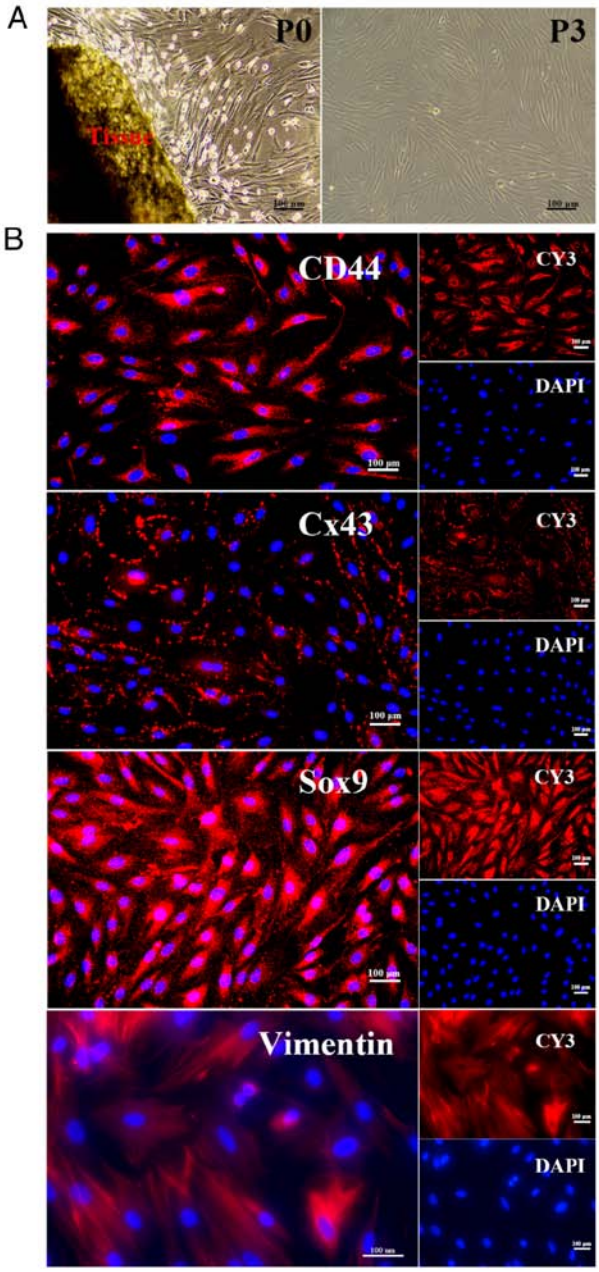

Figure 1. Morphology and fluorescence identification of EMSCs. (A) EMSCs in P0 and P3. (B) Expression of MSC markers (CD44, Vimentin) and neural crest-related biomarkers (Cx43, Sox9). EMSCs, ectodermal mesenchymal stem cells; Sox9, SRY-related high-mobility group box-containing protein 9; Cx43, Connexin43.

Aerosol inhalation of EMSC-Sec improves ALI. The mice in the EMSC-Sec group received pretreatment with an atomizer. After injection of LPS, the mice continued to receive aerosol inhalation of EMSC-Sec for 24 h (Fig. 4A). All ALI mice exhibited obvious arching of the back and less activity. Mice in the treatment group exhibited more activity and sleek fur

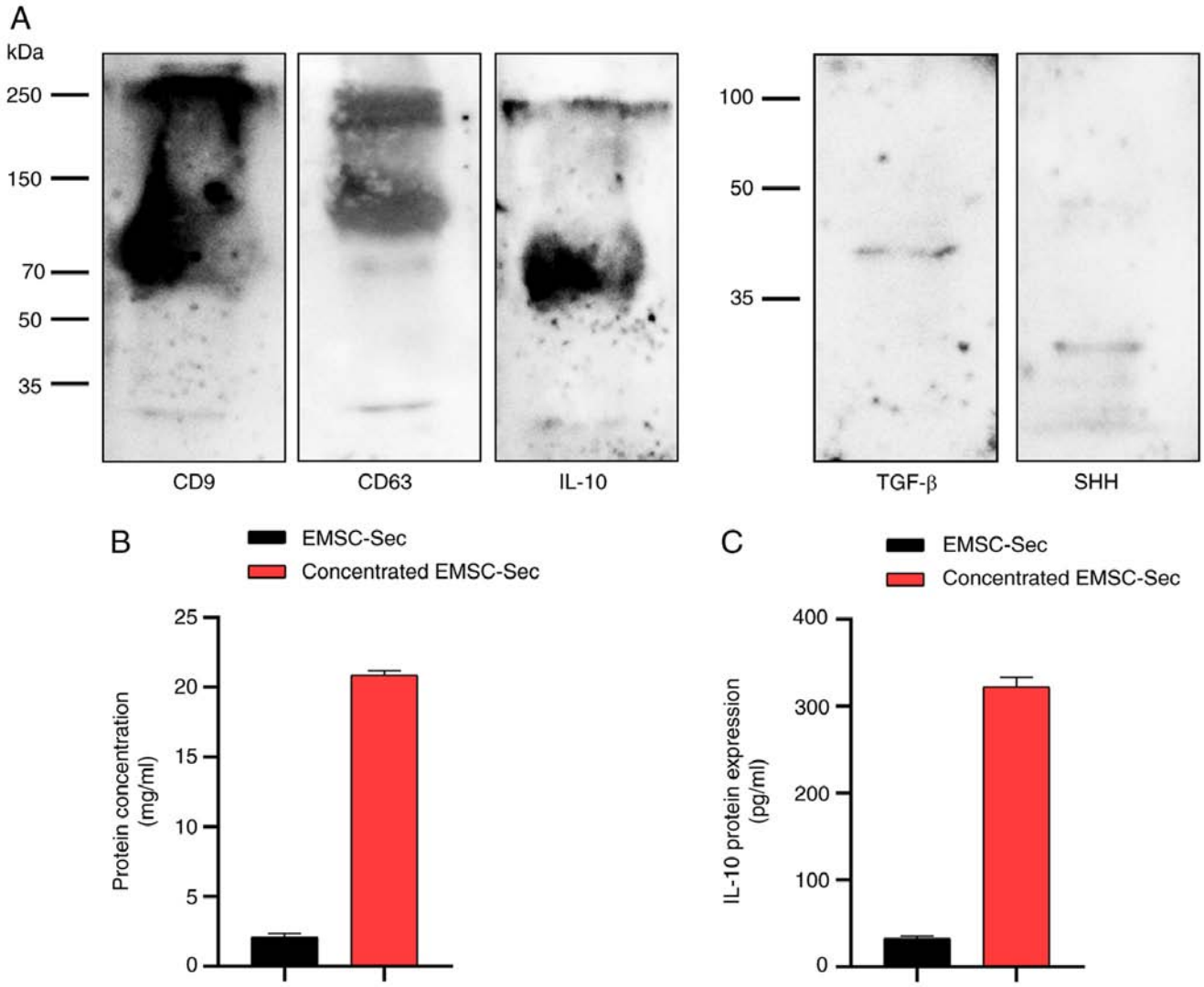

Figure 2. Therapeutic potential of EMSC-Sec. (A) Analysis of IL-10, TGF-β, Sonic hedgehog (SHH), CD9 and CD63 in Ectodermal mesenchymal stem cell-Sectome (EMSC-Sec) by western blotting. (B) Protein concentration of EMSC-Sec (directly collected from EMSCs) and concentrated EMSC-Sec (10-fold enrichment). (C) IL-10 in different forms of EMSC-Sec. SHH, Sonic hedgehog; EMSC-Sec, ectodermal mesenchymal stem cell-Sectome.

compared with LPS group. Morphological observation of the lung, liver and spleen showed that the lung was swollen and the surface of the liver was coarse and dull under the LPS challenge (Fig. 4B). Notably, EMSC-Sec improved this phenomenon. Furthermore, we observed a darker appearance in the spleens of both the LPS and the EMSC-Sec group. Splenic melanosis in mice is a reflex of melanogenesis in the skin, which is unrelated to the inflammatory disease (41,42). W/D ratio demonstrated that EMSC-Sec could reduce the degree of pulmonary edema significantly (Fig. 4D). H&E staining showed that the alveolar structure was destroyed and numerous inflammatory cells infiltrated the LPS group (Fig. 4C). However, EMSC-Sec reversed this phenomenon. EMSC-Sec significantly decreased lung damage score, suggesting a positive effect of EMSC-Sec in ALI (Fig. 4E).

EMSC-Sec protects the lung via inhibiting inflammation. Immunohistochemical staining demonstrated that the EMSC-Sec group exhibited good morphological structure and low expression of IL-17, indicating decreased inflammation (Fig. 5).

EMSC-Sec regulates the inflammatory response at the protein level. ELISA showed that EMSC-Sec inhibited the inflammatory cytokines (TNF-α) and upregulated anti-inflammatory cytokines (IL-10; Fig. 6B-C). Myeloperoxidase (MPO), which has proven to be a local mediator of tissue injury, causes various inflammatory diseases (43). Dysregulation of TNF-α is a hallmark of inflammatory disease (44). EMSC-Sec prevented the induction of MPO and TNF-α in LPS-induced ALI, revealing the anti-inflammatory effect (Fig. 6A). There was an increase in IL-10 in the EMSC-Sec group. Compared with LPS group, lung tissue in the EMSC-Sec group expressed lower levels of MPO and TNF-α (Fig. 6D and E), which may be due to the significant increase of IL-10 (Fig. 6G). Additionally, there was significant upregulation of SHH following LPS stimulation, which may be due to tissue injury. Compared with the EMSC-Sec group, the LPS group had higher levels of SHH, indicating that the mice in the LPS group had more lesions (Fig. 6F).

Upregulation of IL-10 suppresses inflammation in ALI. To explore the association between IL-10 and TNF-α,

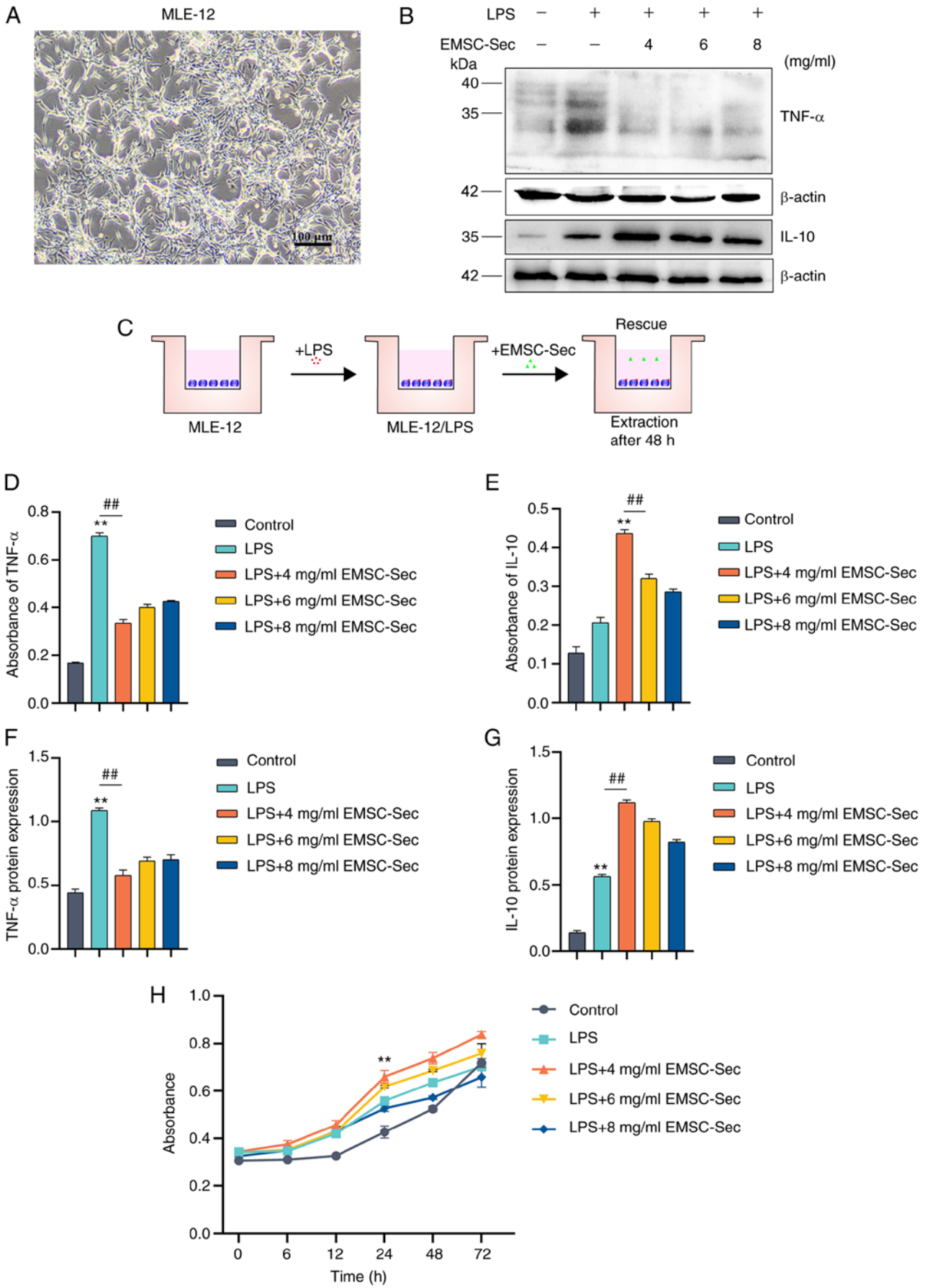

Figure 3. Effects of EMSC-Sec in MLE-12 cells following LPS challenge. (A) Morphological characteristics of MLE-12 cells. (B) Western blotting. (C) Schematic diagram of *in vitro* investigations involving EMSC-Sec. (D and E) ELISA of (D) TNF-α and (E) IL-10 (n=2/group). Quantification of western blotting of (F) TNF-α and (G) IL-10 (n=3/group). Data are means ± SEM. **P<0.01 vs. control; $^{\#\#}$P<0.01. (H) Cell Counting Kit-8 tests *in vitro* (n=3/group). **P<0.01 vs. LPS. EMSC-Sec, ectodermal mesenchymal stem cell-Sectome; LPS, lipopolysaccharide.

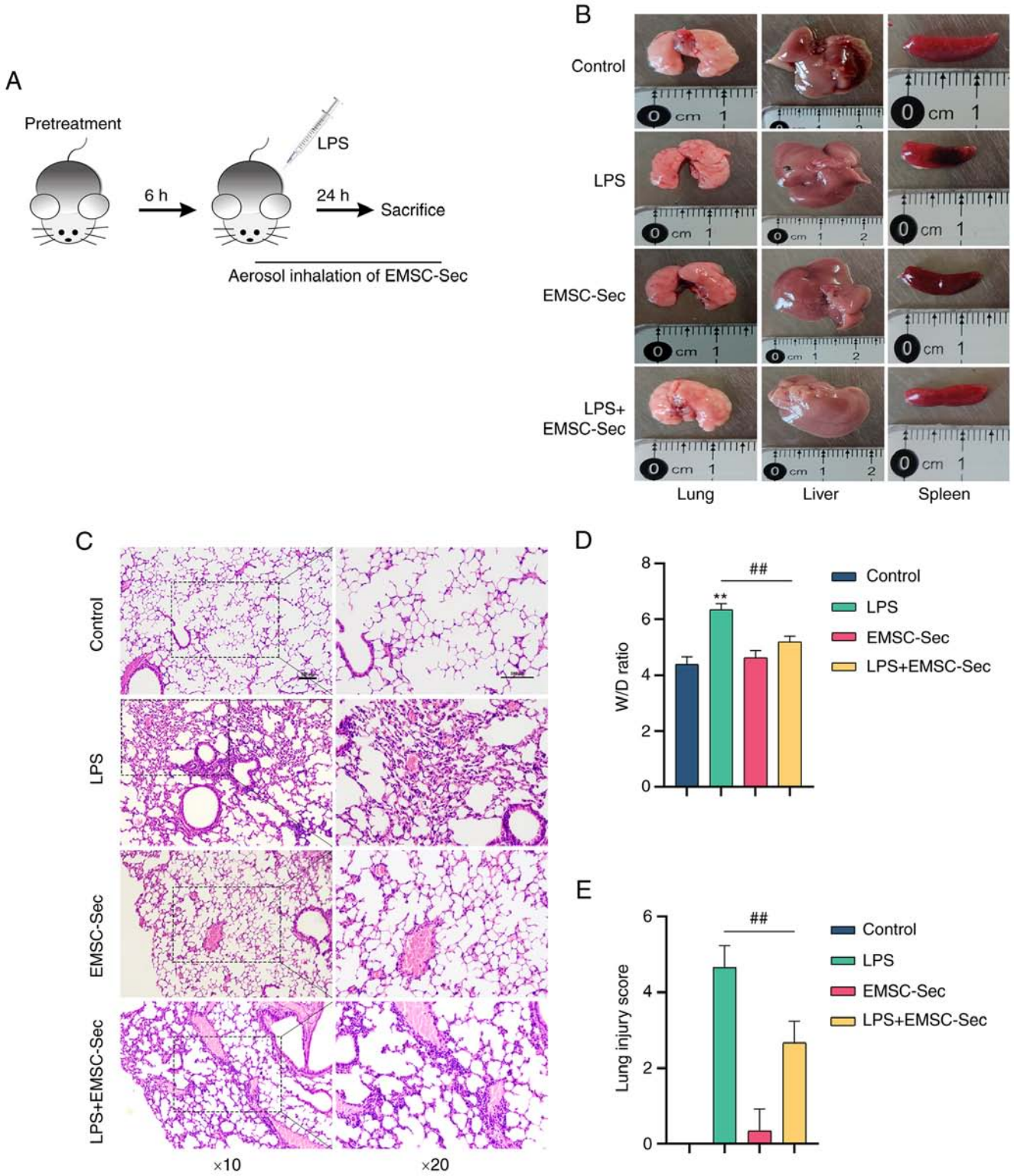

Figure 4. EMSC-Sec improves ALI. (A) Experimental design of *in vivo* study. (B) Tissues (lung, liver, spleen) were collected. (C) H&E staining of lung tissue sections. (D) Lung W/D ratio of LPS-induced ALI mice (n=3). (E) Lung injury scores according to H&E staining (n=3). The data are expressed as mean ± SEM. **P<0.01 vs. control; $^{\#\#}$P<0.01. EMSC-Sec, ectodermal mesenchymal stem cell-Sectome; ALI, acute lung injury; H&E, hematoxylin and eosin; W/D, wet/dry; LPS, lipopolysaccharide.

immunofluorescence was performed. LPS and EMSC-Sec groups expressed increased IL-10 in the injury site (Fig. 7). Of note, EMSC-Sec group expressed higher levels of IL-10 compared with the LPS group. Moreover, the EMSC-Sec group provided better protection to lung tissue structure and reduced TNF-α levels. IL-10 within inflammatory lesions resulted in subdued TNF-α expression, implying that the increased IL-10 levels induced by EMSC-Sec had an inhibitory effect on inflammation.

EMSC-Sec inhibits inflammation via the NF-κB(p50/p65)/NLRP3 pathway. EMSC-Sec significantly inhibited the

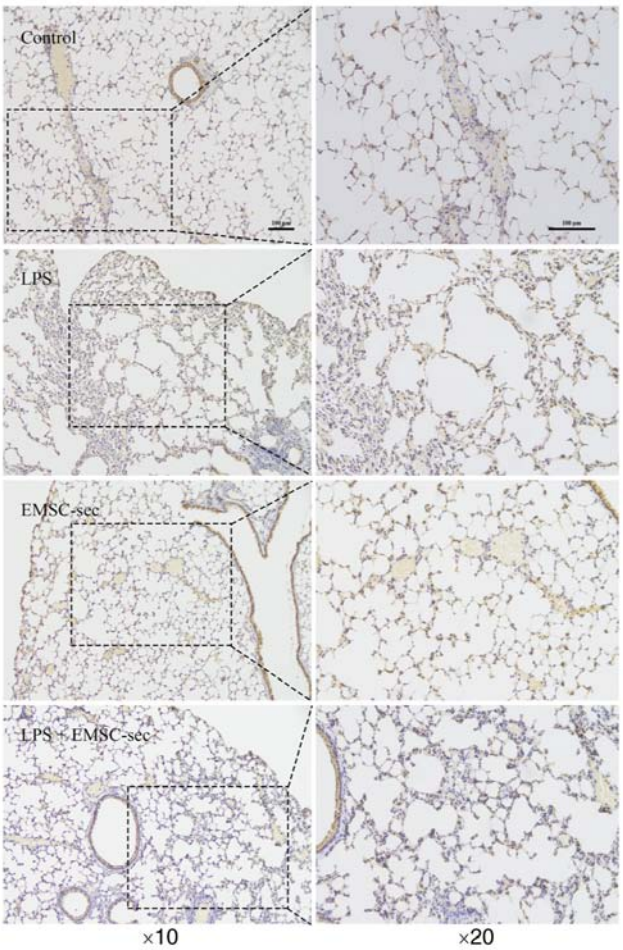

Figure 5. Representative immunohistochemical staining for detection of IL-17. EMSC-Sec, ectodermal mesenchymal stem cell-Sectome; LPS, lipopolysaccharide.

inflammatory response in ALI. The anti-inflammatory effect may not be due to changes in IL-10 alone. NF-κB(p50/p65) disorder typically results in uncontrolled inflammation (22). LPS stimulation increased the expression of TLR4 which is a component of Gram-negative bacteria, to induce the production of pro-inflammatory mediators and kill bacteria (Fig. 8A) (45). EMSC-Sec restored the balance of NF-κB (p50/p65) and IκB following LPS treatment (Fig. 8B and C). EMSC-Sec also decreased the expression of NF-κB (Fig. 8C) and increased p-IκB (Fig. 8B). Relative to the LPS group, NLRP3 was significantly inhibited by EMSC-Sec (Fig. 8D), which demonstrated the anti-inflammatory properties of EMSCs-Se. Fig. 8E illustrates the mechanism by which EMSC-Sec operates. Briefly, Inhibiting IKB phosphorylation by EMSC-Sec diminishes NF-κB (P50/P65) activation, resulting in a lowered inflammation level.

Discussion

The present study investigated whether EMSC-Sec possesses an anti-inflammatory influence *in vitro* and *in vivo*. EMSC-Sec improved inhibited inflammation by increasing IL-10 and proliferation of MLE-12 cells. Additionally, EMSC-Sec performed biological functions to regulate LPS-induced ALI. EMSC-Sec efficiently controlled the inflammatory conditions and triggered an increase in IL-10 levels upon arrival at the site of lung injury. EMSC-Sec was also found to inhibit the NF-κB(p50/p65)/NLRP3 pathway, contributing to down-regulation of inflammatory cytokines *in vivo*. Collectively, the present study demonstrated therapeutic effects of EMSC-Sec in ALI and the underlying mechanism.

The pandemic caused by severe acute respiratory distress syndrome coronavirus 2 (SARS-CoV-2) provided novel insight into the host's reaction to infections and cytokine storms (46). As a disease associated with host immune response, severe sepsis leads to a cascade of production of cytokines (47). The uncontrolled production of cytokines seriously threatens human health in sepsis (48,49). Acute respiratory distress syndrome caused by sepsis directly results in high mortality (35-45%) (50). Although drugs such as antibiotics, antiviral medications, and vasodilators have been developed, there is still a lack of effective treatment methods (51).

Recently, mesenchymal stem cells (MSCs) have been the subject of investigation due to their ability to modulate the immune system and their trophic activity (19). Many researchers posit that the bioactive molecules released by MSCs could potentially reshape the local microenvironment where the lesion is located (52,53). Thus, MSCs-Sec may be a therapeutic option for inflammatory diseases.

Inhaled aerosols are a promising candidate for delivering drugs for lung disease due to rapid achievement of high tissue concentrations after application (54). Aerosolized medication exhibits encouraging results in lung diseases (55-57). For example, when adelmidrol is administered via aerosol, it effectively diminishes oxidative stress and mitigates inflammatory damage in cases of ALI (58). However, the effects of EMSC-Sec on sepsis-induced ALI are unclear. The present study investigated the role of EMSC-Sec in regulating inflammation in ALI. EMSC-Sec limited inflammation and improved ALI. IL-10 serves an essential role in combating damage caused by inflammation. Previous studies have reported that IL-10 maintains tissue homeostasis by restricting excessive inflammatory responses and promoting damaged tissue regeneration (59,60). The potent immunosuppressive capabilities of IL-10 are ascribed to its role as a target for both the innate and adaptive immune responses during the infection resolution phase (61,62). IL-10 may be an effective strategy for autoimmune diseases such as rheumatoid arthritis (63), psoriasis (64), allergic asthma (65) and inflammatory bowel disease (66). Therefore, the present study evaluated levels of IL-10 in ALI. While EMSC-Sec may have anti-inflammatory potential, the anti-inflammatory effects of EMSC-Sec in ALI are unknown (67). IL-17 is a key proinflammatory cytokine in the T helper 17 pathway (68). IL-17 levels are elevated in various inflammatory conditions, including sepsis, pneumonia, systemic lupus erythematosus, rheumatoid arthritis, allograft rejection and cancer (69). Thus, the detection of IL-17 could be meaningful. Increased IL-10 suggested the anti-inflammation potential of EMSC-Sec and may explain the lower levels of inflammatory cytokines, especially IL-17, in the LPS + EMSC-Sec group. Quiescence in the adult lung is an actively maintained state and is regulated by hedgehog signaling. Hedgehog controls epithelial quiescence and regeneration in response to injury via a mesenchymal feedback mechanism (70). The current investigation identified exogenous SHH within EMSC-Sec, showcasing its therapeutic relevance

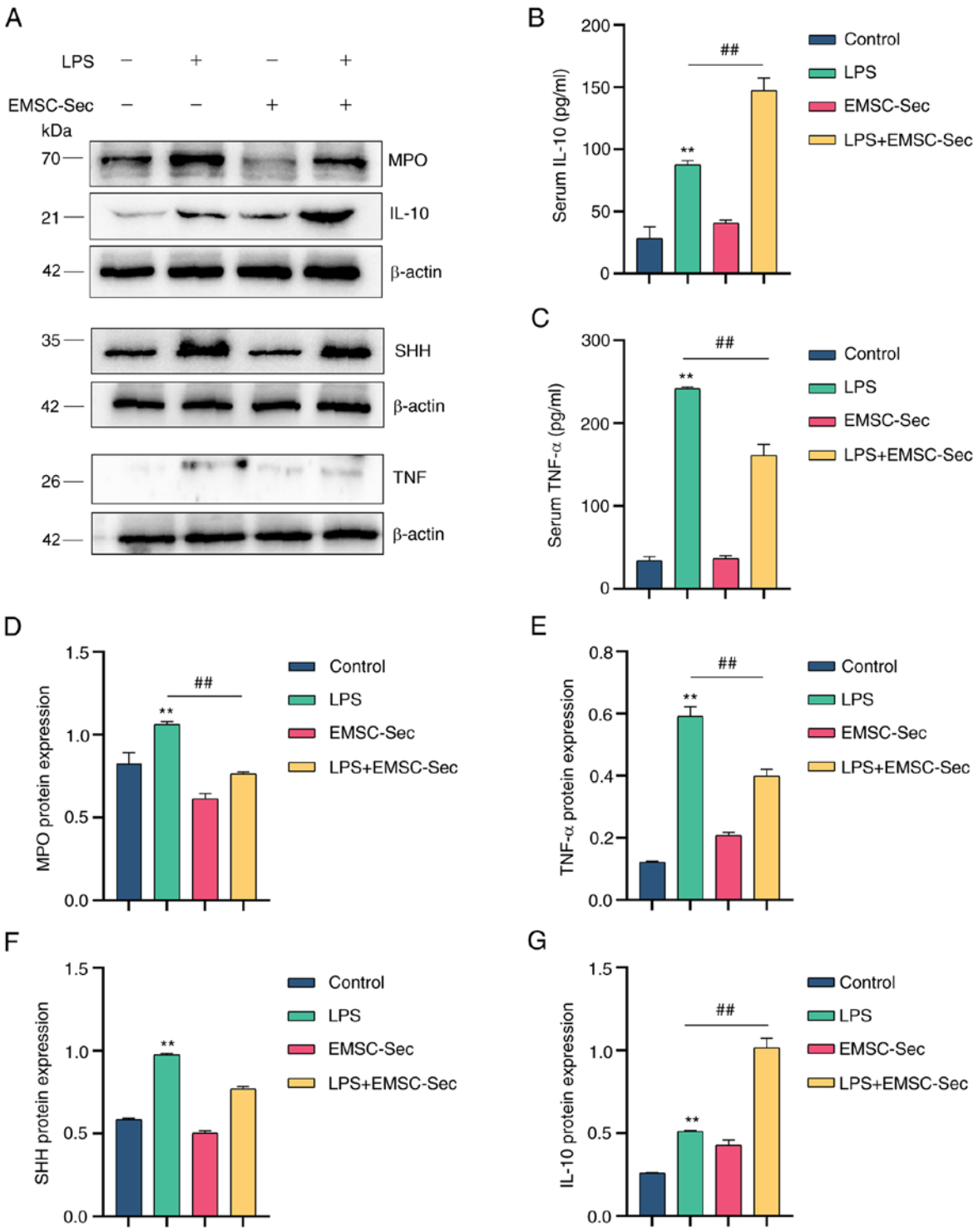

Figure 6. EMSC-Sec decreases pro-inflammatory cytokines produced by LPS. (A) Expression of MPO, TNF-α, IL-10, and SHH in mice using western blotting. Levels of (B) IL-10 and (C) TNF-α in serum using ELISA (n=3 in each group). Protein levels of (D) MPO, (E) TNF-α, (F) SHH and (G) IL-10, and SHH following LPS treatment (n=3/group). **P<0.01 vs. control; $^{##}$P<0.01. EMSC-Sec, ectodermal mesenchymal stem cell-Sectome; LPS, lipopolysaccharide; MPO, myeloperoxidase; SHH, Sonic hedgehog.

due to its capacity for regeneration. SHH is a morphogen that regulates tissue development during embryogenesis (71). Here, SHH was also elevated obviously in the LPS + EMSC-Sec group. This may be associated with active components (MicroRNA125b) and exosomes (72,73). EMSC-Sec interfered with nuclear localization of NF-κB(p50/p65) and ultimately inhibited the NF-κB(p50/p65)/NLRP3 pathway. Aberrant activation of NLRP3 inflammation is associated with pathogenesis of various inflammatory conditions. NLRP3 inflammasome can activate pyroptosis and ultimately induce the inflammatory cytokines storm (74). Fragile signals from NLRP3 not only directly reduce the release of the proinflammatory cytokines IL-1β and IL-18 but also dampen Gasdermin D (GSDMD)-mediated pyroptosis, thereby preventing widespread inflammation (75). EMSC-Sec-induced NLRP3 suppression may also explain low levels of inflammation in the EMSC-Sec group. The upregulation

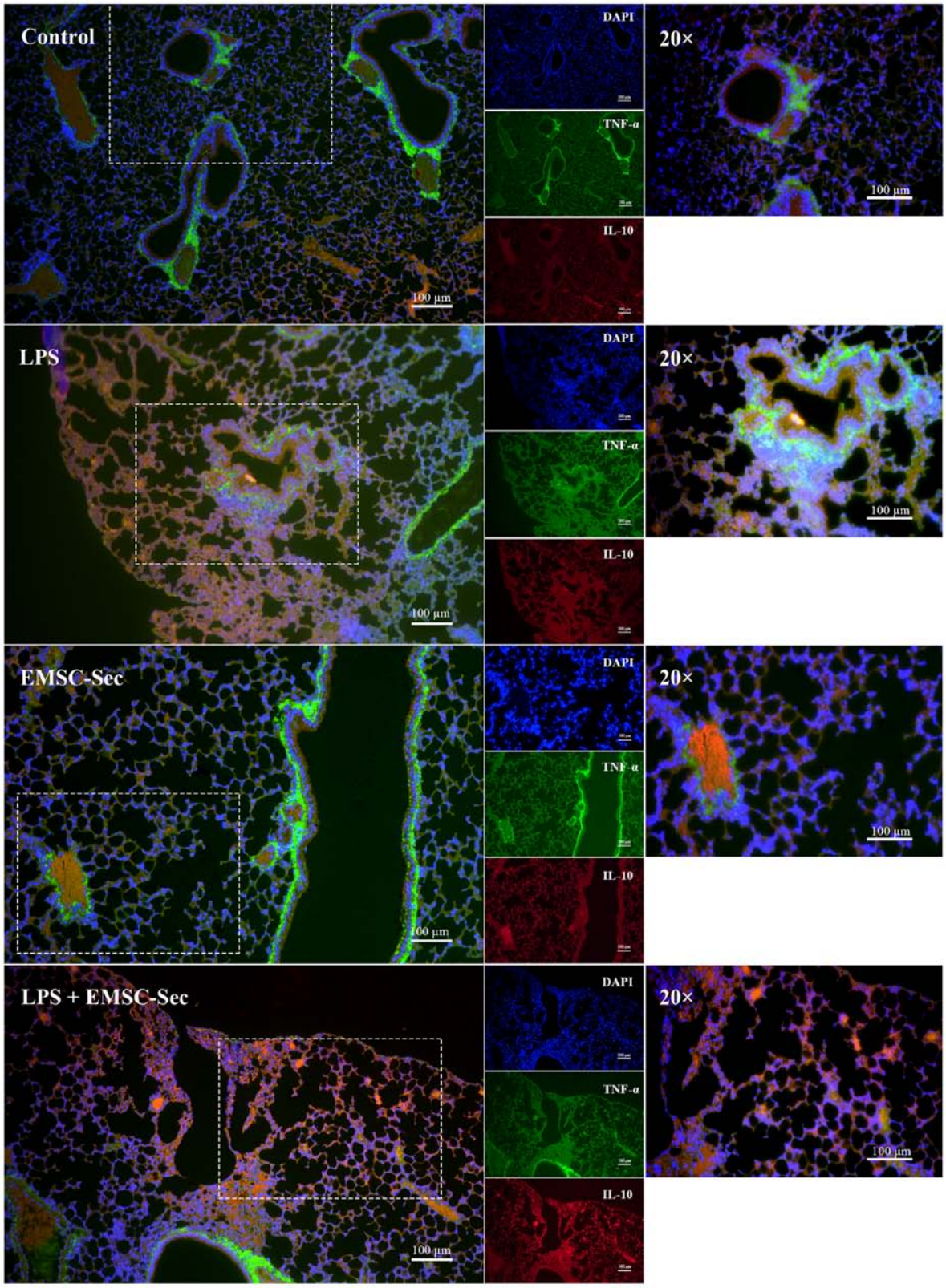

Figure 7. Enhancement of IL-10 suppresses inflammation. Representative immunofluorescence. EMSC-Sec, ectodermal mesenchymal stem cell-Sectome; LPS, lipopolysaccharide.

of IL-10 and NF-κB(p50/p65)/NLRP3 pathway inhibition may explain how EMSC-Sec inhibits inflammatory cytokine storm.

Non-invasive inhalation of EMSC-Sec aims to open up new possibilities for clinical treatment. Here, EMSC-Sec could alleviate LPS-induced ALI via decreasing inflammatory cytokines. However, the mechanism needs to be confirmed due to the complex components. Expression of p-IκB in the LPS + EMSC-Sec group was less than that in the control group. Under physiological conditions, the body is in equilibrium and protein expression is stable. LPS and EMSC-Sec

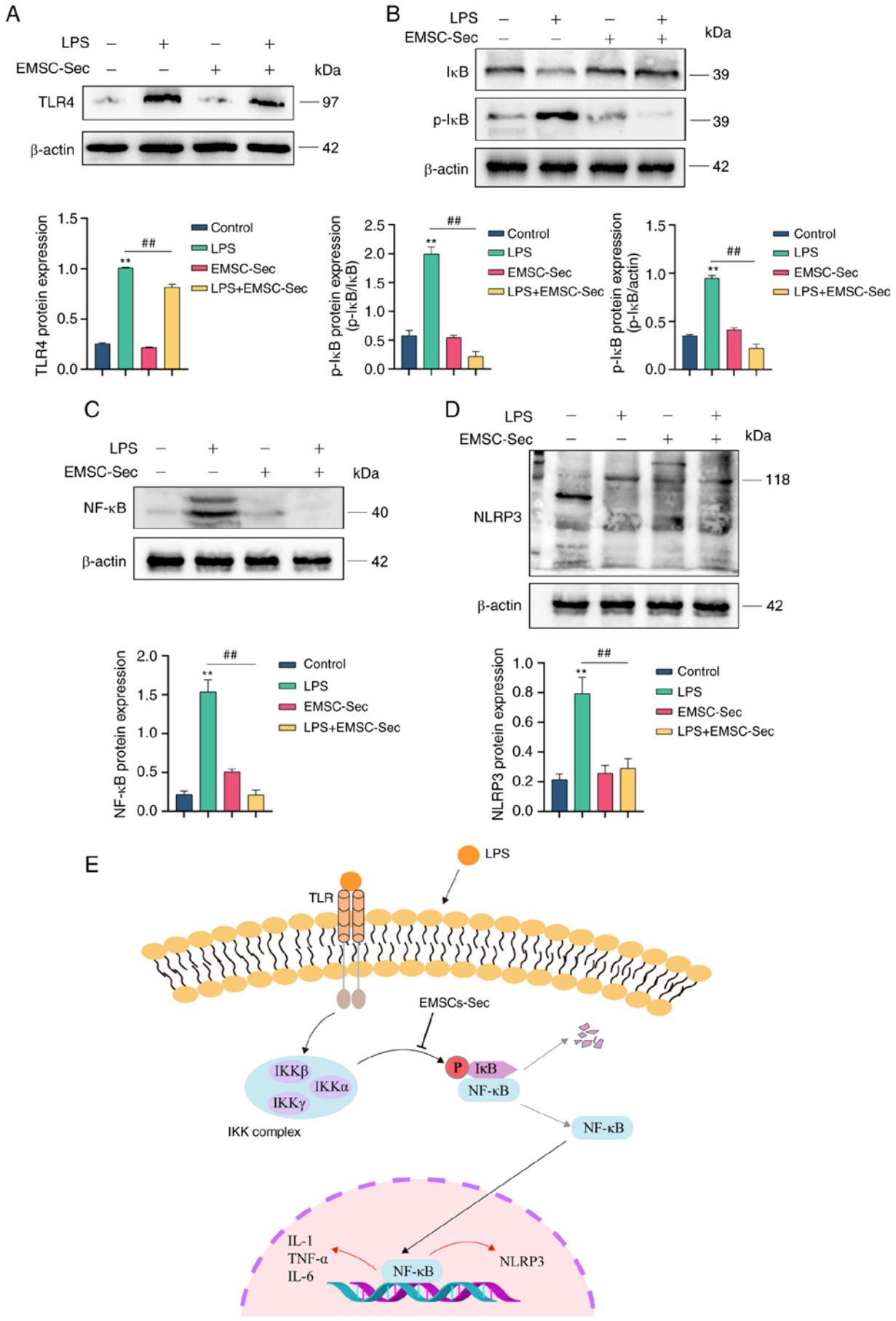

Figure 8. Effects of EMSC-Sec on NF-κB(p50/p65)/NLRP3 pathway signaling in lung tissue of acute lung injury. Western blotting of (A) TLR4, (B) IκB and p-IκB, (C) NF-κB(p50/p65) and (D) NLRP3 in mice (n=3). (E) Schematic illustration of mechanisms of NF-κB(p50/p65)/NLRP3 pathway. **P<0.01 vs. control; $^{\#\#}$P<0.01. EMSC-Sec, ectodermal mesenchymal stem cell-Sectome; LPS, lipopolysaccharide; TLR, Toll-like receptors; p-, phosphorylated.

act as separate influencing factors disrupting the equilibrium. LPS disrupts the inflammatory balance of the body. This inflammatory stress response induces transient overexpression of IκB. EMSC-Sec induces a second inflammatory stress response because of its potent anti-inflammation effects (76). This response may account for low expression of IκB in the LPS + EMSC-Sec group. Proinflammatory proptosis caused by inflammatory activation frequently triggers cytokine storms (77,78). While EMSC-Sec achieved anti-inflammatory effects in ALI, the relationship between EMSC-Sec and pyroptosis remains to be studied.

Acknowledgements

Not applicable.

Funding

The present study was supported by the Technology Project of 'Ke Jiao Xing Wei' in Suzhou City (grant no. KJXW2020066).

Availability of data and materials

The datasets used and/or analyzed during the present study are available from the corresponding author on reasonable request.

Authors' contributions

JT and FL designed and conceived the study, constructed figures and wrote the manuscript. JT, ZZ and XW collected samples and performed experiments. YQ and YZ analyzed data. All authors have read and approved the final manuscript. JT and FL confirm the authenticity of all the raw data.

Ethics approval and consent to participate

The animal experiments were approved by the animal research institute of Jiangsu University (approval no. UJS-IACUC-2022051901).

Patient consent for publication

Not applicable.

Competing interests

The authors declare that they have no competing interests.

References

1. Zheng Q, Wang YC, Liu QX, Dong XJ, Xie ZX, Liu XH, Gao W, Bai XJ and Li ZF: FK866 attenuates sepsis-induced acute lung injury through c-jun-N-terminal kinase (JNK)-dependent autophagy. Life Sci 250: 117551, 2020.
2. Tang D, Wang H, Billiar TR, Kroemer G and Kang R: Emerging mechanisms of immunocoagulation in sepsis and septic shock. Trends Immunol 42: 508-522, 2021.
3. Zhao B, Lu R, Chen J, Xie M, Zhao X and Kong L: S100A9 blockade prevents lipopolysaccharide-induced lung injury via suppressing the NLRP3 pathway. Respir Res 22: 45, 2021.
4. Wu C, Li H, Zhang P, Tian C, Luo J, Zhang W, Bhandari S, Jin S and Hao Y: Lymphatic flow: A potential target in sepsis-associated acute lung injury. J Inflamm Res 13: 961-968, 2020.
5. Zhang Y, Yu W, Han D, Meng J, Wang H and Cao G: L-lysine ameliorates sepsis-induced acute lung injury in a lipopolysaccharide-induced mouse model. Biomed Pharmacother 118: 109307, 2019.
6. Zhou M, Fang H, Du M, Li C, Tang R, Liu H, Gao Z, Ji Z, Ke B and Chen XL: The modulation of regulatory T cells via HMGB1/PTEN/β-catenin axis in LPS induced acute lung injury. Front Immunol 10: 1612, 2019.
7. Weiss ARR and Dahlke MH: Immunomodulation by mesenchymal stem cells (MSCs): Mechanisms of action of living, apoptotic, and dead MSCs. Front Immunol 10: 1191, 2019.
8. Loke XY, Imran SAM, Tye GJ, Wan Kamarul Zaman WS and Nordin F: Immunomodulation and regenerative capacity of MSCs for long-COVID. Int J Mol Sci 22: 12421, 2021.
9. Fu Y, Ni J, Chen J, Ma G, Zhao M, Zhu S, Shi T, Zhu J, Huang Z, Zhang J and Chen J: Dual-functionalized MSCs that express CX3CR1 and IL-25 exhibit enhanced therapeutic effects on inflammatory bowel disease. Mol Ther 28: 1214-1228, 2020.
10. Wu W, Xiao ZX, Zeng D, Huang F, Wang J, Liu Y, Bellanti JA, Olsen N and Zheng SG: B7-H1 promotes the functional effect of human gingiva-derived mesenchymal stem cells on collagen-induced arthritis murine model. Mol Ther 28: 2417-2429, 2020.
11. Meng F, Xu R, Wang S, Xu Z, Zhang C, Li Y, Yang T, Shi L, Fu J, Jiang T, *et al*: Human umbilical cord-derived mesenchymal stem cell therapy in patients with COVID-19: A phase 1 clinical trial. Signal Transduct Target Ther 5: 172, 2020.
12. Zhu R, Yan T, Feng Y, Liu Y, Cao H, Peng G, Yang Y, Xu Z, Liu J, Hou W, *et al*: Mesenchymal stem cell treatment improves outcome of COVID-19 patients via multiple immunomodulatory mechanisms. Cell Res 31: 1244-1262, 2021.
13. Liu S, Liu F, Zhou Y, Jin B, Sun Q and Guo S: Immunosuppressive property of MSCs mediated by cell surface receptors. Front Immunol 11: 1076, 2020.
14. Hu C, Wu Z and Li L: Mesenchymal stromal cells promote liver regeneration through regulation of immune cells. Int J Biol Sci 16: 893-903, 2020.
15. L PK, Kandoi S, Misra R, S V, K R and Verma RS: The mesenchymal stem cell secretome: A new paradigm towards cell-free therapeutic mode in regenerative medicine. Cytokine Growth Factor Rev 46: 1-9, 2019.
16. Phan J, Kumar P, Hao D, Gao K, Farmer D and Wang A: Engineering mesenchymal stem cells to improve their exosome efficacy and yield for cell-free therapy. J Extracell Vesicles 7: 1522236, 2018.
17. Wechsler ME, Rao VV, Borelli AN and Anseth KS: Engineering the MSC secretome: A hydrogel focused approach. Adv Healthc Mater 10: e2001948, 2021.
18. Chang C, Yan J, Yao Z, Zhang C, Li X and Mao HQ: Effects of mesenchymal stem cell-derived paracrine signals and their delivery strategies. Adv Healthc Mater 10: e2001689, 2021.
19. Song N, Scholtemeijer M and Shah K: Mesenchymal stem cell immunomodulation: Mechanisms and therapeutic potential. Trends Pharmacol Sci 41: 653-664, 2020.
20. Jakob M, Hemeda H, Janeschik S, Bootz F, Rotter N, Lang S and Brandau S: Human nasal mucosa contains tissue-resident immunologically responsive mesenchymal stromal cells. Stem Cells Dev 19: 635-644, 2010.
21. Hong CG, Chen ML, Duan R, Wang X, Pang ZL, Ge LT, Lu M, Xie H and Liu ZZ: Transplantation of nasal olfactory mucosa mesenchymal stem cells benefits Alzheimer's disease. Mol Neurobiol 59: 7323-7336, 2022.
22. Afonina IS, Zhong Z, Karin M and Beyaert R: Limiting inflammation-the negative regulation of NF-κB and the NLRP3 inflammasome. Nat Immunol 18: 861-869, 2017.
23. Halova I, Rönnberg E, Draberova L, Vliagoftis H, Nilsson GP and Draber P: Changing the threshold-Signals and mechanisms of mast cell priming. Immunol Rev 282: 73-86, 2018.
24. Luo B, Huang F, Liu Y, Liang Y, Wei Z, Ke H, Zeng Z, Huang W and He Y: NLRP3 inflammasome as a molecular marker in diabetic cardiomyopathy. Front Physiol 8: 519, 2017.
25. Huang Y, Xu W and Zhou R: NLRP3 inflammasome activation and cell death. Cell Mol Immunol 18: 2114-2127, 2021.
26. He X, Yang W, Zeng Z, Wei Y, Gao J, Zhang B, Li L, Liu L, Wan Y, Zeng Q, *et al*: NLRP3-dependent pyroptosis is required for HIV-1 gp120-induced neuropathology. Cell Mol Immunol 17: 283-299, 2020.
27. Hickey AJ: Emerging trends in inhaled drug delivery. Adv Drug Deliv Rev 157: 63-70, 2020.

28. Sudduth ER, Trautmann-Rodriguez M, Gill N, Bomb K and Fromen CA: Aerosol pulmonary immune engineering. Adv Drug Deliv Rev 199: 114831, 2023.
29. Takaenoki Y, Masui K, Oda Y and Kazama T: The pharmacokinetics of atomized lidocaine administered via the Trachea: A randomized trial. Anesth Analg 123: 74-81, 2016.
30. Shi W, Wang Z, Bian L, Wu Y, HuiYa M, Zhou Y, Zhang Z, Wang Q, Zhao P and Lu X: Periodic heat stress licenses EMSC differentiation into osteoblasts via YAP signaling pathway activation. Stem Cells Int 2022: 3715471, 2022.
31. Peng W, Chang M, Wu Y, Zhu W, Tong L, Zhang G, Wang Q, Liu J, Zhu X, Cheng T, *et al*: Lyophilized powder of mesenchymal stem cell supernatant attenuates acute lung injury through the IL-6-p-STAT3-p63-JAG2 pathway. Stem Cell Res Ther 12: 216, 2021.
32. Lainé A, Labiad O, Hernandez-Vargas H, This S, Sanlaville A, Léon S, Dalle S, Sheppard D, Travis MA, Paidassi H and Marie JC: Regulatory T cells promote cancer immune-escape through integrin αvβ8-mediated TGF-β activation. Nat Commun 12: 6228, 2021.
33. Ouyang W, Rutz S, Crellin NK, Valdez PA and Hymowitz SG: Regulation and functions of the IL-10 family of cytokines in inflammation and disease. Annu Rev Immunol 29: 71-109, 2011.
34. Garg C, Khan H, Kaur A, Singh TG, Sharma VK and Singh SK: Therapeutic implications of sonic hedgehog pathway in metabolic disorders: Novel target for effective treatment. Pharmacol Res 179: 106194, 2022.
35. Zhao X, Zhao Y, Sun X, Xing Y, Wang X and Yang Q: Immunomodulation of MSCs and MSC-derived extracellular vesicles in osteoarthritis. Front Bioeng Biotechnol 8: 575057, 2020.
36. Li Y, Huang J, Foley NM, Xu Y, Li YP, Pan J, Redmond HP, Wang JH and Wang J: B7H3 ameliorates LPS-induced acute lung injury via attenuation of neutrophil migration and infiltration. Sci Rep 6: 31284, 2016.
37. Suzuki K, Okada H, Takemura G, Takada C, Tomita H, Yano H, Muraki I, Zaikokuji R, Kuroda A, Fukuda H, *et al*: Recombinant thrombomodulin protects against LPS-induced acute respiratory distress syndrome via preservation of pulmonary endothelial glycocalyx. Br J Pharmacol 177: 4021-4033, 2020.
38. Baumgarten G, Knuefermann P, Wrigge H, Putensen C, Stapel H, Fink K, Meyer R, Hoeft A and Grohé C: Role of Toll-like receptor 4 for the pathogenesis of acute lung injury in Gram-negative sepsis. Eur J Anaesthesiol 23: 1041-1048, 2006.
39. Shaaban AA, El-Kashef DH, Hamed MF and El-Agamy DS: Protective effect of pristimerin against LPS-induced acute lung injury in mice. Int Immunopharmacol 59: 31-39, 2018.
40. Zhang X, Zhang P, An L, Sun N, Peng L, Tang W, Ma D and Chen J: Miltirone induces cell death in hepatocellular carcinoma cell through GSDME-dependent pyroptosis. Acta Pharm Sin B 10: 1397-1413, 2020.
41. Plonka PM, Michalczyk D, Popik M, Handjiski B, Slominski A and Paus R: Splenic eumelanin differs from hair eumelanin in C57BL/6 mice. Acta Biochim Pol 52: 433-441, 2005.
42. Michalczyk D, Popik M, Salwinski A and Plonka PM: Extradermal melanin transfer? Lack of macroscopic spleen melanization in old C57BL/6 mice with de-synchronized hair cycle. Acta Biochim Pol 56: 343-353, 2009.
43. Davies MJ: Myeloperoxidase: Mechanisms, reactions and inhibition as a therapeutic strategy in inflammatory diseases. Pharmacol Ther 218: 107685, 2021.
44. van Loo G and Bertrand MJM: Death by TNF: A road to inflammation. Nat Rev Immunol 23: 289-303, 2023.
45. Płóciennikowska A, Hromada-Judycka A, Borzęcka K and Kwiatkowska K: Co-operation of TLR4 and raft proteins in LPS-induced pro-inflammatory signaling. Cell Mol Life Sci 72: 557-581, 2015.
46. Fajgenbaum DC and June CH: Cytokine storm. N Engl J Med 383: 2255-2273, 2020.
47. Chousterman BG, Swirski FK and Weber GF: Cytokine storm and sepsis disease pathogenesis. Semin Immunopathol 39: 517-528, 2017.
48. Kumar V: Toll-like receptors in sepsis-associated cytokine storm and their endogenous negative regulators as future immunomodulatory targets. Int Immunopharmacol 89: 107087, 2020.
49. Kim JS, Lee JY, Yang JW, Lee KH, Effenberger M, Szpirt W, Kronbichler A and Shin JI: Immunopathogenesis and treatment of cytokine storm in COVID-19. Theranostics 11: 316-329, 2021.
50. Matthay MA, Zemans RL, Zimmerman GA, Arabi YM, Beitler JR, Mercat A, Herridge M, Randolph AG and Calfee CS: Acute respiratory distress syndrome. Nat Rev Dis Primers 5: 18, 2019.
51. Huang M, Cai S and Su J: The pathogenesis of sepsis and potential therapeutic targets. Int J Mol Sci 20: 5376, 2019.
52. Asgari Taei A, Khodabakhsh P, Nasoohi S, Farahmandfar M and Dargahi L: Paracrine effects of mesenchymal stem cells in ischemic stroke: Opportunities and challenges. Mol Neurobiol 59: 6281-6306, 2022.
53. Tran C and Damaser MS: Stem cells as drug delivery methods: Application of stem cell secretome for regeneration. Adv Drug Deliv Rev 82-83: 1-11, 2015.
54. Fröhlich E and Salar-Behzadi S: Oral inhalation for delivery of proteins and peptides to the lungs. Eur J Pharm Biopharm 163: 198-211, 2021.
55. Gelfand CA, Sakurai R, Wang Y, Liu Y, Segal R and Rehan VK: Inhaled vitamin A is more effective than intramuscular dosing in mitigating hyperoxia-induced lung injury in a neonatal rat model of bronchopulmonary dysplasia. Am J Physiol Lung Cell Mol Physiol 319: L576-L584, 2020.
56. Lee WH, Loo CY, Traini D and Young PM: Development and evaluation of paclitaxel and curcumin dry powder for inhalation lung cancer treatment. Pharmaceutics 13: 9, 2020.
57. Sakurai R, Lee C, Shen H, Waring AJ, Walther FJ and Rehan VK: A combination of the aerosolized PPAR-γ agonist pioglitazone and a synthetic surfactant protein B peptide mimic prevents hyperoxia-induced neonatal lung injury in rats. Neonatology 113: 296-304, 2018.
58. Interdonato L, D'amico R, Cordaro M, Siracusa R, Fusco R, Peritore AF, Gugliandolo E, Crupi R, Coaccioli S, Genovese T, *et al*: Aerosol-administered adelmidrol attenuates lung inflammation in a murine model of acute lung injury. Biomolecules 12: 1308, 2022.
59. Ouyang W and O'Garra A: IL-10 family cytokines IL-10 and IL-22: From basic science to clinical translation. Immunity 50: 871-891, 2019.
60. Saraiva M, Vieira P and O'Garra A: Biology and therapeutic potential of interleukin-10. J Exp Med 217: e20190418, 2020.
61. Engelhardt KR and Grimbacher B: IL-10 in humans: Lessons from the gut, IL-10/IL-10 receptor deficiencies, and IL-10 polymorphisms. Curr Top Microbiol Immunol 380: 1-18, 2014.
62. Mollazadeh H, Cicero AFG, Blesso CN, Pirro M, Majeed M and Sahebkar A: Immune modulation by curcumin: The role of interleukin-10. Crit Rev Food Sci Nutr 59: 89-101, 2019.
63. Chen Z, Bozec A, Ramming A and Schett G: Anti-inflammatory and immune-regulatory cytokines in rheumatoid arthritis. Nat Rev Rheumatol 15: 9-17, 2019.
64. Asadullah K, Döcke WD, Sabat RV, Volk HD and Sterry W: The treatment of psoriasis with IL-10: Rationale and review of the first clinical trials. Expert Opin Investig Drugs 9: 95-102, 2000.
65. Tumes DJ, Papadopoulos M, Endo Y, Onodera A, Hirahara K and Nakayama T: Epigenetic regulation of T-helper cell differentiation, memory, and plasticity in allergic asthma. Immunol Rev 278: 8-19, 2017.
66. Koelink PJ, Bloemendaal FM, Li B, Westera L, Vogels EWM, van Roest M, Gloudemans AK, van't Wout AB, Korf H, Vermeire S, *et al*: Anti-TNF therapy in IBD exerts its therapeutic effect through macrophage IL-10 signalling. Gut 69: 1053-1063, 2020.
67. Wang Z, Zhang X, Qi L, Feng W, Gu Y and Ding Y: Olfactory mucosa tissue-derived mesenchymal stem cells lysate ameliorates LPS-induced acute liver injury in mice. BMC Pulm Med 22: 414, 2022.
68. Tan HL and Rosenthal M: IL-17 in lung disease: Friend or foe? Thorax 68: 788-790, 2013.
69. Ge Y, Huang M and Yao YM: Biology of interleukin-17 and its pathophysiological significance in sepsis. Front Immunol 11: 1558, 2020.
70. Peng T, Frank DB, Kadzik RS, Morley MP, Rathi KS, Wang T, Zhou S, Cheng L, Lu MM and Morrisey EE: Hedgehog actively maintains adult lung quiescence and regulates repair and regeneration. Nature 526: 578-582, 2015.
71. Pepicelli CV, Lewis PM and McMahon AP: Sonic hedgehog regulates branching morphogenesis in the mammalian lung. Curr Biol 8: 1083-1086, 1998.
72. Hyun J, Wang S, Kim J, Kim GJ and Jung Y: MicroRNA125b-mediated Hedgehog signaling influences liver regeneration by chorionic plate-derived mesenchymal stem cells. Sci Rep 5: 14135, 2015.

73. Qi J, Zhou Y, Jiao Z, Wang X, Zhao Y, Li Y, Chen H, Yang L, Zhu H and Li Y: Exosomes derived from human bone marrow mesenchymal stem cells promote tumor growth through hedgehog signaling pathway. Cell Physiol Biochem 42: 2242-2254, 2017.
74. Zhao N, Di B and Xu LL: The NLRP3 inflammasome and COVID-19: Activation, pathogenesis and therapeutic strategies. Cytokine Growth Factor Rev 61: 2-15, 2021.
75. Coll RC, Schroder K and Pelegrín P: NLRP3 and pyroptosis blockers for treating inflammatory diseases. Trends Pharmacol Sci 43: 653-668, 2022.
76. Latour A, Gu Y, Kassis N, Daubigney F, Colin C, Gausserès B, Middendorp S, Paul JL, Hindié V, Rain JC, *et al*: LPS-induced inflammation abolishes the effect of DYRK1A on IkB stability in the brain of mice. Mol Neurobiol 56: 963-975, 2019.
77. Wei Y, Yang L, Pandeya A, Cui J, Zhang Y and Li Z: Pyroptosis-induced inflammation and tissue damage. J Mol Biol 434: 167301, 2021.
78. de Vasconcelos NM and Lamkanfi M: Recent insights on inflammasomes, gasdermin pores, and pyroptosis. Cold Spring Harb Perspect Biol 12: a036392, 2020.